J Appl Electrochem (2008) 38:197–202
DOI 10.1007/s10800-007-9424-z

ORIGINAL PAPER

Electrochemical hydriding/dehydriding of nanocrystalline $Mg_{2-x}Sn_xNi$ (x = 0, 0.1, 0.3)

Nikola Drenchev · Tony Spassov · Ivan Kanazirski

Received: 15 June 2007 / Revised: 10 September 2007 / Accepted: 14 September 2007 / Published online: 2 October 2007

Abstract The electrochemical hydriding/dehydriding under galvanostatic conditions of nanostructured $Mg_{2-x}Sn_xNi$ (x = 0,0.1,0.3) were studied at different temperatures in the range 28–45 °C. The discharge capacity, cycle life and electrochemical impedance of the alloys were found to depend on the presence of Sn. Tin decreases the maximum electrochemical capacity, but essentially improves the cycle life of Mg_2Ni. Intensive corrosion of surface Mg was found to take place during the first 2–3 charge/discharge cycles to a much larger extent for Mg_2Ni, compared to the tin containing alloys. Sn decreases the electron density around the Mg atoms and therefore impedes magnesium oxidation. It was also found that Sn hampers charge transfer but reduces the hydrogen diffusion resistance in Mg_2Ni based alloys.

Keywords Magnesium alloys · Tin · Nanocrystalline · Ball milling · Electrochemical charge/discharge · Impedance

1 Introduction

Mg_2Ni-based alloys and composites are among the most studied magnesium materials for hydrogen storage [1–7]. The hydriding properties of Mg_2Ni based alloys depend on the microstructure and the type and amount of the alloying elements. The hydriding/dehydriding temperature of Mg_2Ni alloy can be decreased by adding Al, V, or Mn [8–11]. The cycle life of the alloys in electrochemical charge/discharge tests can be increased by replacing part of Mg with Ti, Al, Co, Ce, Cr or Sn [12–15]. Reducing the particle and grain size of Mg-based alloys improves the hydrogen capacity and hydriding/dehydriding kinetics [3, 7, 16, 17].

Although the influence of different alloying elements and microstructure on the electrochemical capacity, cycle life and corrosion of Mg_2Ni-based materials has been extensively studied various questions concerning the mechanism of this influence are still not explained. Our recent study [15] revealed enhanced microstructural refinement of Sn containing Mg_2Ni alloys during ball milling combined with improved cycle life of the electrode, prepared from $Mg_{2-x}Sn_xNi$. Thus, the aim of the present study was to investigate the influence of Sn on the electrochemical hydriding/dehydriding characteristics of $Mg_{2-x}Sn_xNi$ (x = 0,0.1,0.3).

2 Experimental details

$Mg_{2-x}Sn_xNi$ (x = 0, 0.1, 0.3) alloys were synthesized by ball milling. The experimental conditions of the alloy preparation were described previously [15]. The alloys were characterized by means of SEM (JEOL JSM-5510), X-ray diffraction with Cu-K_α radiation, XPS and EDS. Electrochemical hydriding/dehydriding experiments were carried out in a three electrode cell with Hg/HgO as a reference electrode and a counter electrode prepared from Ni mesh. The metal hydride electrode was prepared by mixing the alloy powder (100 mg) with 70 mg Teflonyzed carbon black (VULCAN 72 10%PTFE) and pressing the as-prepared mixture with a pressure of 1250 kg cm^{-2}. Pellets with a diameter of 10 mm and thickness of about

N. Drenchev · T. Spassov (✉)
Department of Chemistry, University of Sofia "St.Kl.Ohridski",
1 J. Bourchier str., Sofia 1164, Bulgaria
e-mail: tspassov@chem.uni-sofia.bg

I. Kanazirski
University of Chemical Technology and Metallurgy, Sofia,
Bulgaria

1.5 mm were obtained. The electrolyte was 6 M KOH water solution. Electrochemical charging and discharging was conducted at constant current of 0.1 A g^{-1} and 0.01 A g^{-1}, respectively. The cut off voltage was 400 mV versus reference electrode. Electrochemical impedance (IE) measurements were carried out with an Autolab PGSTAT 30 in the frequency range 50 kHz to 0.01 Hz and amplitude of 15 mV.

3 Results and discussion

The morphology and microstructure of the $Mg_{2-x}Sn_xNi$ (x = 0, 0.1, 0.3) alloys studied were considered in our previous work [15]. Although at these concentrations Sn does not result in a new phase formation its addition shifts the position of the diffractions peaks to larger angles (Fig. 1), indicating a reduction into the lattice parameters of the hexagonal Mg_2Ni. The average composition of the tin containing alloys was determined using EDS analyzer and was found to correspond to the nominal composition of the alloys.

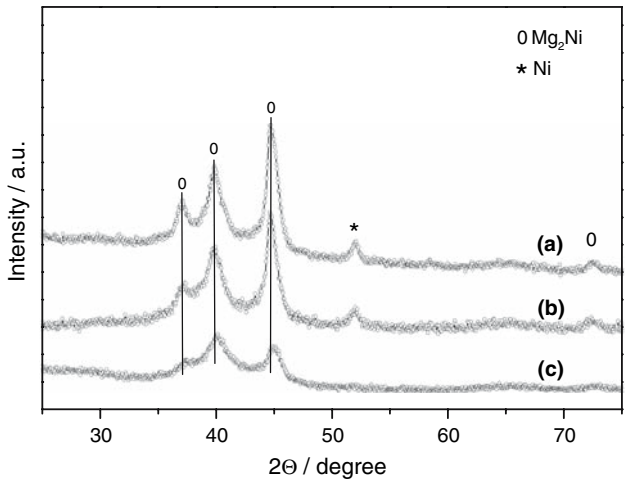

Fig. 1 XRD patterns of the ball milled (**a**) Mg_2Ni, (**b**) $Mg_{1.9}Sn_{0.1}Ni$ and (**c**) $Mg_{1.7}Sn_{0.3}Ni$ alloys

The XPS spectra of Mg (Fig. 2) show that the binding energy is shifted to a higher value for the $Mg_{1.7}Sn_{0.3}Ni$ alloy compared to Mg_2Ni. Obviously, Sn decreases the electron density around Mg atoms and it can be suggested that charge transfer and oxidation of Mg on the alloy surface is impeded.

3.1 Electrochemical hydriding/dehydriding

Figure 3a and b present hydrogen charge curves of electrodes prepared from Mg_2Ni and $Mg_{1.7}Sn_{0.3}Ni$ alloys at 28 °C. As will be shown later the electrochemical sorption of hydrogen completes in the nonlinear part of the charge curves. A visible difference in the shape of the charge curves of the two alloys can be detected. For Mg_2Ni a stepped voltage increase is observed during charging, whereas the charging curves of $Mg_{1.7}Sn_{0.3}Ni$ show a continuous potential increase. The amount of tin in $Mg_{1.9}Sn_{0.1}Ni$ alloy is not enough to change the type of the hydrogen charge curves and they look similar to those of the Mg_2Ni alloy; therefore they are not presented in Fig. 3. The discharge curves of the alloys are shown in Fig. 4. $Mg_{1.9}Sn_{0.1}Ni$ showed highest discharge capacity of 359 mAh g^{-1}. The cycle life of the electrodes is presented in Fig. 5. It can be concluded that the amount of absorbed hydrogen decreases with cycle number. The increased Sn and decreased Mg content improve the cycle life of the electrode, as $Mg_{1.7}Sn_{0.3}Ni$ possesses the highest corrosion stability among the three alloys studied.

Mg_2Ni and $Mg_{1.7}Sn_{0.3}Ni$ alloys were charged and discharged at different temperatures. The capacity change with the cycle number for the two alloys at different temperatures is shown in Figs. 6 and 7. The discharge capacity of Mg_2Ni increases with temperature and at 45 °C reaches 480 mAh g^{-1}. At this temperature however a drastic decrease in the corrosion stability of the alloy was observed. Similar cycle life behavior with temperature increase was observed for the $Mg_{1.7}Sn_{0.3}Ni$ alloy (Fig. 7). The highest initial capacity for Mg_2Ni was measured at the

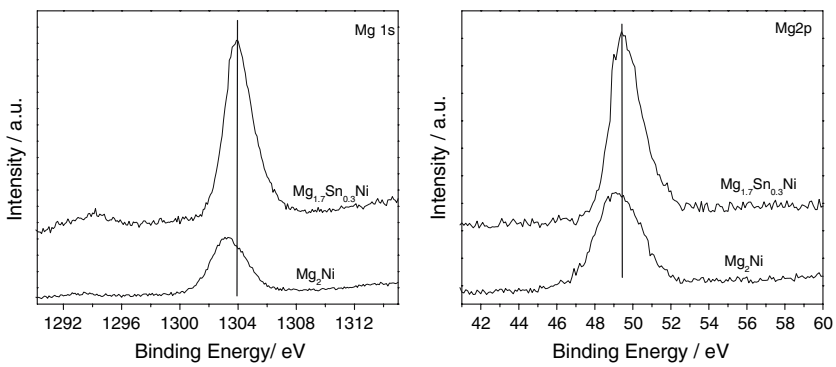

Fig. 2 Mg 1s,2p spectra of Mg_2Ni and $Mg_{1.7}Sn_{0.3}Ni$ alloys

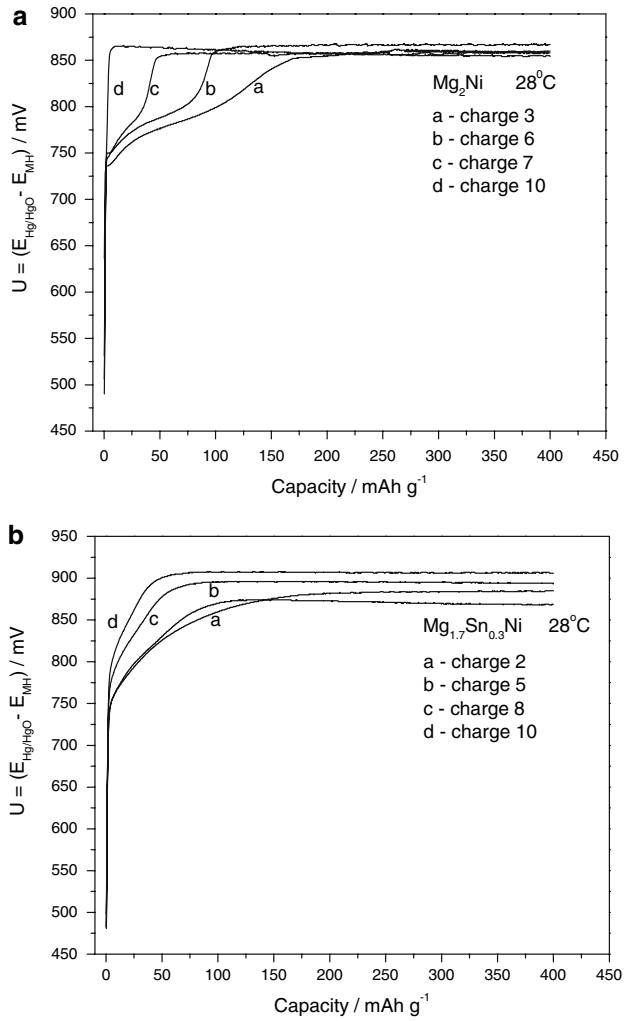

Fig. 3 (**a**) Charge curves of Mg_2Ni (charged with 10 mA for 4 h). (**b**) Charge curves of $Mg_{1.7}Sn_{0.3}Ni$ (charged with 10 mA for 4 h)

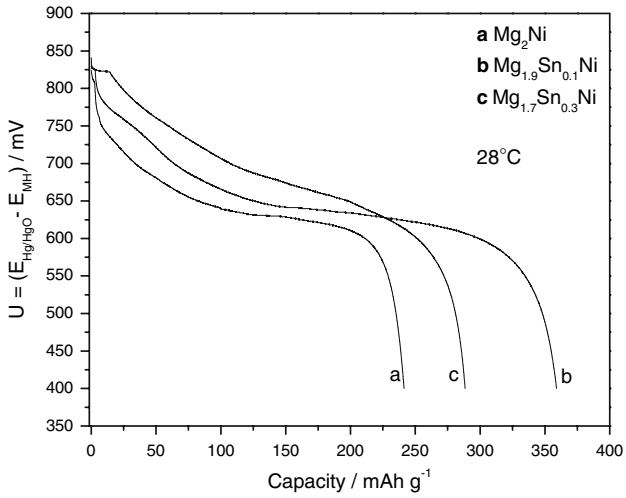

Fig. 4 Discharge curves of (**a**) Mg_2Ni, (**b**) $Mg_{1.9}Sn_{0.1}Ni$ and (**c**) $Mg_{1.7}Sn_{0.3}Ni$ alloys

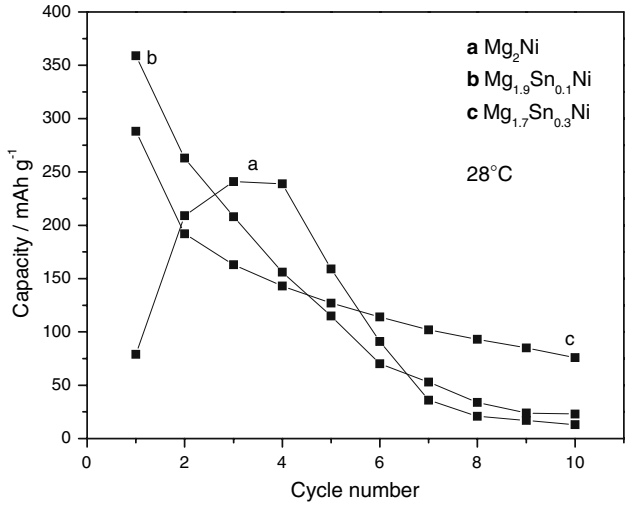

Fig. 5 Cycle life of the electrodes prepared from (**a**) Mg_2Ni, (**b**) $Mg_{1.9}Sn_{0.1}Ni$ and (**c**) $Mg_{1.7}Sn_{0.3}Ni$ alloys

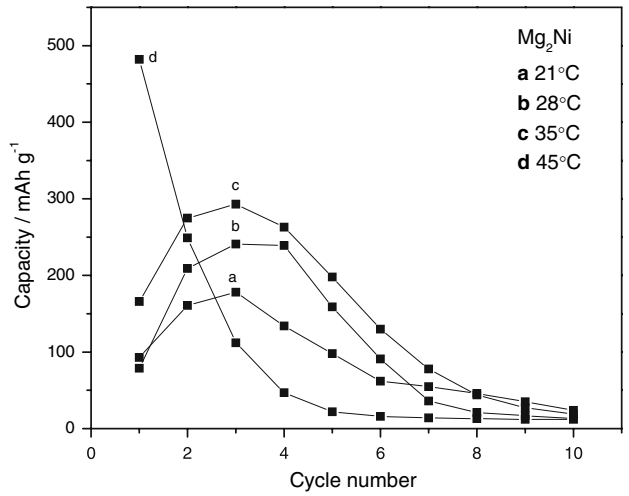

Fig. 6 Cycle life of the electrodes prepared from Mg_2Ni at different temperatures

highest temperature (45 °C) and at the same time the cycle life was the worst. At lower temperatures (≤35 °C) a capacity maximum is observed around the 3rd charge/discharge cycle. Generally, at all temperatures studied the corrosion stability of the Sn-containing alloys is higher compared to the pure Mg_2Ni. This result is in agreement with XPS analysis, indicating impeded oxidation of Mg on the particle surface due to the presence of Sn.

However, the initial discharge capacity obtained at 45 °C for both alloys is higher than the maximum possible, determined from the charge curves. This finding called for a careful analysis of the discharge curves. Figure 8 shows the first discharge curve of the electrode prepared from Mg_2Ni at 45 °C. Two distinct steps at different potentials are clearly registered, revealing that two different processes

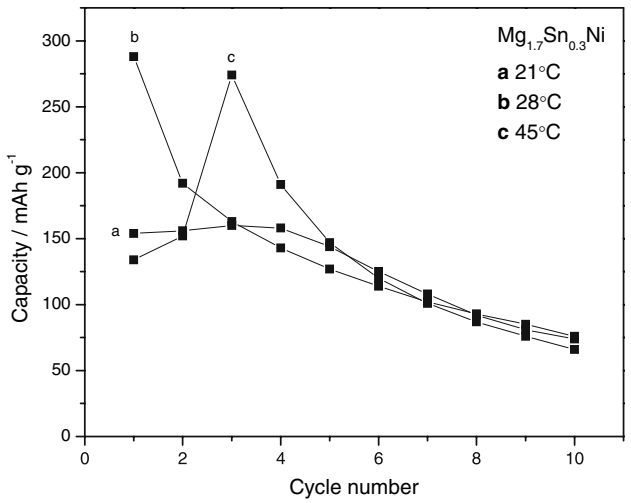

Fig. 7 Cycle life of the electrodes prepared from $Mg_{1.7}Sn_{0.3}Ni$ at different temperatures

take place. Since the charge time was 4 h at a current density of 0.1 A g^{-1} if we assume that the whole amount of electricity is consumed for the reduction of H^+ to H atoms (i.e. 100% charge efficiency) then the maximum discharge capacity appears to be 400 mAh g^{-1}. The charge curve is not presented in Fig. 8, because during the first charging the electrolyte does not penetrate the entire electrode volume directly. Thus the effective area of the electrode changes continuously, which has an influence on the voltage value measured. Therefore correct determination of the amount of absorbed hydrogen is not possible. Taking into account the above arguments it can be suggested that the first step in the discharge process is the following reaction, taking place on the alloy surface:

$$Mg - 2e^- \rightarrow Mg^{2+} \quad (1)$$

This process is irreversible in aqueous solution. The magnesium ions on the alloy surface react with OH^- to form $Mg(OH)_2$. Simultaneously, the reaction

$$2H - 2e^- \rightarrow 2H^+ \quad (2)$$

takes place, but its contribution to the overall capacity in this range of potentials is negligible. The next step in the "U–t" curve is associated with reaction (2). This explains the capacity above 400 mAh g^{-1}, determined from the discharge curve. Charge and discharge curves at the second cycle for Mg_2Ni are shown in Fig. 9. The amount of absorbed hydrogen, determined from the charge curve, corresponds to the discharge capacity. During the second discharge the first potential step is almost missing, because the larger part of Mg on the alloy surface is already oxidized. For the $Mg_{1.7}Sn_{0.3}Ni$ alloy two potential steps are also observed in the discharge curve, Fig. 10. For this alloy the charge capacity is about 120–150 mAh g^{-1} and the discharge capacity is 274 mAh g^{-1}. The observed difference in this case also results from the above described processes.

3.2 Electrochemical impedance spectroscopy

The kinetics of hydrogen transfer and hydrogen diffusion in the bulk of $Mg_{2-x}Sn_xNi$ (x = 0, 0.1, 0.3) alloys have been investigated using electrochemical impedance spectroscopy. Typical Nyquist plots of the three alloys at 100% and 0% state of charge (SOC) are shown in Figs. 11 and 12. There are three regions related to the electrochemical reaction resistance (charge transfer) on the surface between the

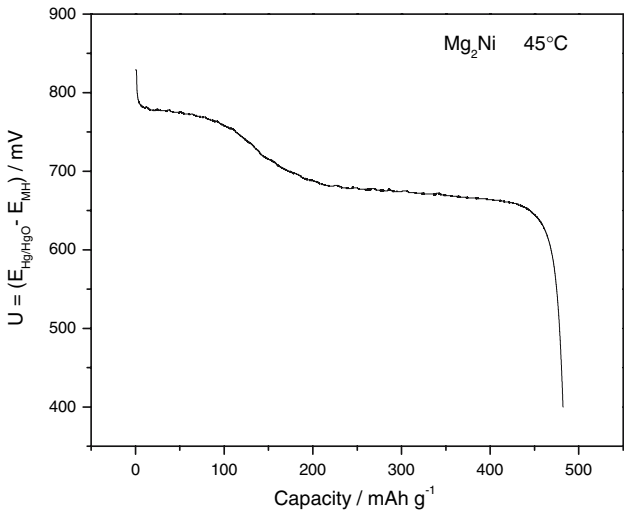

Fig. 8 First discharge curve of the electrode prepared from Mg_2Ni alloy at 45 °C

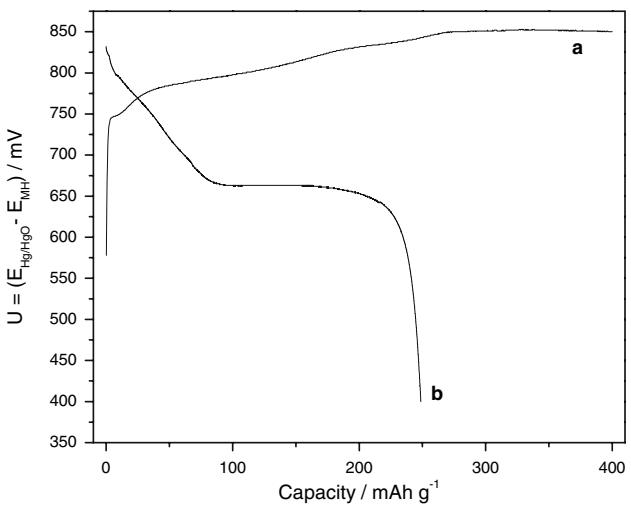

Fig. 9 Second charge curve (**a**) and second discharge curve (**b**) of the electrode prepared from Mg_2Ni alloy at 45 °C

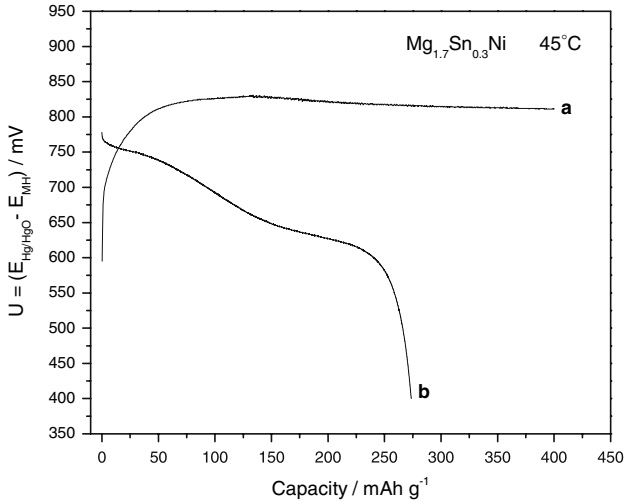

Fig. 10 Third charge curve (**a**) and third discharge curve (**b**) of the electrode prepared from $Mg_{1.7}Sn_{0.3}Ni$ alloy

electrode and electrolyte (larger distorted semicircle), hydrogen adsorption (second semicircle) and a linear region related to hydrogen diffusion in the bulk of the alloys. The resistance related to the charge transfer reaction increases with increasing Sn content. Table 1 shows the angle coefficient calculated from the linear part of the Nyquist plot from 0.77526 to 0.02206 Hz. The angle coefficient (slope) for $Mg_{1.7}Sn_{0.3}Ni$ alloy is the lowest compared to the other two alloys, which indicates that Sn reduces the diffusion resistance. Since a slight reductuion of the Mg_2Ni lattice parameters was detected when adding Sn (see Fig. 1) the increased hydrogen diffusivity in $Mg_{1.7}Sn_{0.3}Ni$ compared to that in Mg_2Ni is most probably due to finer microstructure of the former alloy.

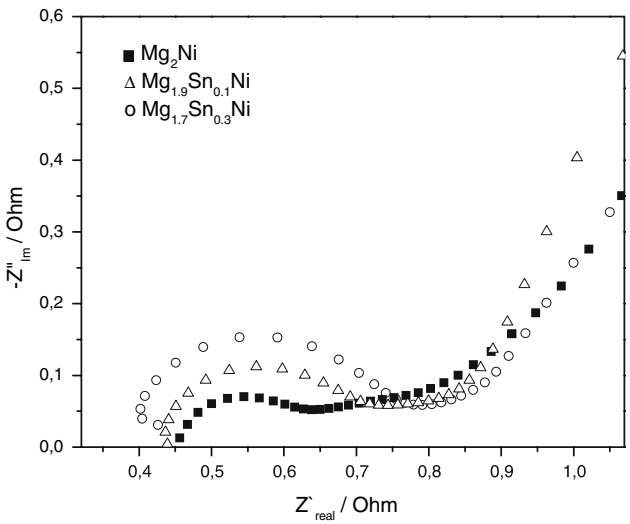

Fig. 11 Nyquist plot of Mg_2Ni (charge 3), $Mg_{1.9}Sn_{0.1}Ni$ (charge 4) and $Mg_{1.7}Sn_{0.3}Ni$ (charge 4) alloy at 100% SOC

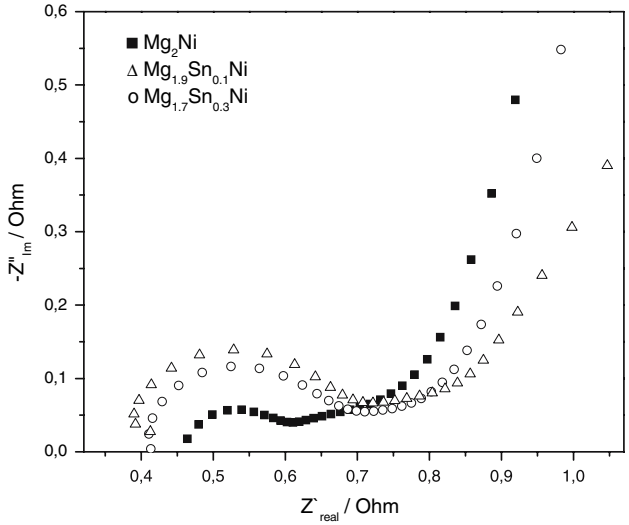

Fig. 12 Nyquist plot of Mg_2Ni (discharge 2), $Mg_{1.9}Sn_{0.1}Ni$ (discharge 3) and $Mg_{1.7}Sn_{0.3}Ni$ (discharge 3) alloy at 0% SOC

Table 1 Slopes, calculated from the linear part of the Nyquist plot (from 0.77526 Hz to 0.02206 Hz) in Figs. 11 and 12

Alloy	$\Delta(-Z'')/\Delta$ (Z') at 20 °C, 100% SOC	$\Delta(-Z'')/\Delta$ (Z' at 20 °C, 0% SOC
Mg_2Ni	1.23 ± 0.04	6.34 ± 0.14
$Mg_{1.9}Sn_{0.1}Ni$	1.59 ± 0.05	5.15 ± 0.10
$Mg_{1.7}Sn_{0.3}Ni$	0.85 ± 0.07	3.82 ± 0.12

4 Conclusion

The influence of Sn on the electrochemical hydrogen capacity, cycle life and electrochemical impedance of nanocrystalline $Mg_{2-x}Sn_xNi$ ($x = 0$, 0.1, 0.3) alloys was studied. Generally, tin slightly reduces the discharge capacity, but improves the cycle life of the alloys at all temperatures studied (21–45 °C). An electron density decrease around the magnesium atoms due to the presence of Sn in the alloy was detected, which was assumed to result in Mg oxidation impediment. Another possible reason for the cycle life improvement of $Mg_{2-x}Sn_xNi$ could be a change in the composition and structure of the corrosion product on the electrode surface in the presence of Sn. It was also found that Sn impedes the charge transfer, but facilitates the hydrogen adsorption process and reduces the hydrogen diffusion resistance in Mg_2Ni based alloys.

Acknowledgment The work was supported by the Bulgarian Scientific Research Fund under grant BYX-14/05 and by the National Science Fund, Project "University research center on nanotechnologies and new materials".

References

1. Niu H, Northwood DO (2002) Int J Hydrogen Energy 27:69
2. Yuan H, Li Q, Song H, Wang Y, Lui J (2003) J Alloys Compd 353:322
3. Orimo S, Fujii H (2001) Appl Phys A 72:167
4. Liang G, Huot J, Boily S, Van Neste A, Schulz R (1999) J Alloys Compd 282:286
5. Li Q, Chou KC, Xu KD, Lin Q, Jiang LJ, Zhan F (2006) Intermetallics 14(12):1386
6. Tojo T, Yamamoto I, Zhang Q, Saito F (2005) Adv Powder Technol 16(6):649
7. Han SS, Lee HY, Goo NH, Jeong WT, Lee KS (2002) J Alloys Compd 330–332:841
8. Kohno T, Kanda M (1997) J Electrochem Soc 144(7):2384
9. Nohara S, Hamasaki K, Zhang SG, Inoue H, Iwacura C (1998) J Alloys Compd 280:104
10. Delchev P, Solsona P, Drenchev B, Drenchev N, Spassov T, Baro MD (2005) J Alloys Compd 388:98
11. Grigorova E, Khristov M, Khrussanova M, Peshev P (2006) J Alloys Compd 414:298
12. Zhang Y, Chen LX, Lei YQ, Wang QD (2002) J Electrochimica Acta 47:1739
13. Orimo S, Zuttel A, Ikeda K, Saruki S, Fukunaga T, Fujii H, Schlapbach L (1999) J Alloys Compd 295:437
14. Ruggeri S, Ruoe L, Huot J, Schulz R, Aymard L, Tarascon JM (2002) J Power Sources 112:547
15. Drenchev N, Spassov T, Bliznakov S (2006) J Alloys Compd (in press)
16. Bliznakov S, Drenchev N, Drenchev B, Solsona P, Spassov T (2005) J Alloys Compd 404–406:682
17. Zhu M, Wang ZM, Peng CH, Zeng MQ, Gao Y (2003) J Alloys Compd 349:284